Thermal characterisation of triple tube heat exchangers by parameter estimation approach

Thermal characterisation of triple tube heat exchangers by parameter estimation approach

M Malavasi[a], L Cattani[b*], P Vocale[a], F Bozzoli[a,c], S Rainieri[a,c]

[a] Department of Engineering and Architecture, University of Parma, Parco Area delle Scienze 181/A, Parma, Italy
[b] CIDEA Interdepartmental Centre, University of Parma, Parco Area delle Scienze 181/A, Parma, Italy
[c] SITEIA Interdepartmental Centre, University of Parma, Parco Area delle Scienze 181/A, Parma, Italy

E-mail address of the corresponding Author (Luca Cattani): luca.cattani1@unipr.it

Abstract. A parameter estimation approach was applied to characterise the heat transfer inside a triple tube heat exchanger (TTHE) designed for the food industry. This type of heat transfer device represents a promising technology for the always increasing challenge of reducing the consumption of energy and raw materials. Especially, it provides a suitable solution for the heat treatment of highly viscous fluids; making the product flowing into the intermediate pipe, this kind of heat exchanger permits heat transfer both through the internal and the external surfaces, reducing the device size compared to traditional double tube heat exchangers. Moreover, this configuration reduces the problems related to product stratification, avoiding the risk of having part of the product burned and part not heated enough. However, the thermal design of these apparatuses is critical. Although they present a widespread industrial application, it is difficult to find correlations for their thermal behaviour. This study fills this gap by proposing an effective methodology for deriving a proper heat transfer correlation. Among the different methodologies that can be adopted to assess the performance of the TTHEs, the parameter estimation procedure represents a promising tool since it has been successfully applied in many disciplines of engineering. Following this approach, this study enables the successful and robust estimation of the heat transfer correlation for the product side Nusselt number starting from the temperature measurements at the inlet and outlet sections of the three tubes. The procedure was validated by adopting both synthetic and experimental data acquired from a TTHE for treating highly viscous fluid foods.

Keywords: Triple Tube Heat Exchangers, Parameter Estimation, Nusselt Number Correlation, Highly Viscous Food Fluids

1. Introduction

A triple tube heat exchanger (TTHE) is a modified version of a double tube heat exchanger (DTHE), which comprises adding an intermediate tube to a DTHE. This geometry increases the heat transfer area compared to a double tube because the fluid circulating through the intermediate gap (usually the product) is heated or cooled from both the inner and outer sides of the annulus. Unlike the DTHE, in which the possible flow configurations are two, i.e. parallel flow and counter flow, there are three flows inducing four configurations in a TTHE: counter-current, co-current, counter-current & co-current, and co-current & counter-current [1].

TTHEs are widely used in the food and pharmaceutical industries. In the food industry, this heat exchanger is used for sterilisation, pasteurisation, and cooling treatments; for instance, liquid products such cream and pulpy orange juice are pasteurised using TTHE [2]. Despite the advantages and wide use of TTHEs, especially in cases where the fluid under treatment is highly viscous and exhibits complex rheological behaviour, the scientific literature on this topic contains some gaps, including the thermal design of these apparatuses, as highlighted by Kumar and Hariprasath in their recent review [3]. Moreover, it is difficult to apply the few data available in the literature to TTHEs due to the specificity of each product, thermal treatment, and geometrical configuration, making the thermal design of these apparatuses critical. Therefore, it appears to be more useful to assess the methodology used to derive a proper heat transfer correlation than to assess the form of the heat transfer correlation itself, as the correlation often cannot be transferred to other heat exchangers, even those that belong to the same class.

Generally, the experimental investigations reported in the literature [1–12] aim to measure the average thermal performance of the device for different conditions (different Reynolds number values in the three sections, heating/cooling conditions, etc…) and different geometric configurations, often adopting the effectiveness-NTU method or the log-mean temperature.

Despite the DTHE, in which there are only two fluid flows, the energy of the fluid that flows in the inner annulus is exchanged in two opposite directions in a TTHE (to the fluids in the inner tube and outer annulus);

therefore, the approach based on the evaluation of the logarithmic mean temperature difference is no longer valid.

To overcome this problem, Gomaa et al. [1] introduced an average log-mean temperature difference between the three fluids, defined as the arithmetic mean between the log-mean temperature difference between the fluid in the annulus and the one in the external tube and the log-mean temperature difference between the annulus and internal pipe. The same approach was recently adopted by Tiwari et al. [4].

Another study, Ünal [5,6] conducted a theoretical analysis of this type of heat exchanger, deriving closed form expressions for the effectiveness-NTU relations, including both the counter-flow and parallel flow configurations. Batmaz and Sandeep [7] and Radulescu et al. [8] proposed and developed a procedure that included a calculation algorithm that could determine the overall heat transfer and axial temperature distribution in a TTHE.

Recently, Moya-Rico et al. [9] proposed an alternative tool based on artificial neural networks to accurately predict the heat transfer rate and the pressure drop in a TTHE. By adopting the same approach, Bahiraei et al. [10–12] predicted the overall heat transfer coefficient of a TTHE and investigated heat transfer enhancement due to the insertion of nanofluid and crimpled-spiral ribs.

Even if the experimental data are treated by adopting the dimensional analysis approach due to the specificity of each plant and product treated, it is often difficult to extend the validity of the suggested heat transfer correlations that often hold for the specific geometry under investigation.

Considering the more critical procedure of defining a correlation for heat transfer for TTHEs than the form of correlation itself due to the specificity of any single application case of these devices, this study proposes and validates a data processing procedure intended to characterise TTHEs, which helps in estimating the heat transfer correlation for the product side Nusselt number.

One of the simplest methods used to estimate the inside heat transfer coefficient in heat exchangers is the well-known Wilson plot technique [13]. In this technique, a simple linear curve-fitting procedure was used to estimate both the sum of the wall and shell side resistances and the constant of the internal side heat transfer correlation. Briggs and Young [14] suggested and validated a procedure for determining three unknowns rather than two, as the exponent expressing the power law dependence of the internal Nusselt number on the Reynolds number was also estimated. A more general approach based on a non-linear regression scheme was presented by Khartabil and Christensen [15]. A unified Wilson plot method based on non-linear regression was applied by Styrylska and Lechowska [16]. A general review of the Wilson plot method and its modifications to determine convection coefficients in heat exchanger devices was presented by Rose [17] and Fernández-Seara et al. [18].

However, the application technique proposed by Wilson to TTHE presents some macroscopic problems due to the impossibility of defining a univocal behaviour of the ‘shell’ side: the two sections in which flows the service fluid influence each other, making it difficult to determine a unique thermal resistance for the service side. These limitations of the approach used by Wilson could be overcome as proposed by Gomaa et al. [1] and Pătrăşcioiu et al. [19] by adopting an average log-mean temperature, as previously described.

A promising solution to completely bypass the limitations of the Wilson plot technique can be found in the parameter estimation procedure, which represents a powerful tool for many engineering applications [20, 21]. Particularly, the parameter estimation procedure helps to estimate unknown parameters that play an important role in the design and optimisation of heat transfer devices and heat exchangers that are customised for certain specific purposes, as often happens with TTHE. This methodology has recently been adopted to investigate the performance of DTHE based on the assumption that both internal and external convective heat transfer coefficients can be expressed as a function of the Reynolds and Prandtl numbers [22].

Since the parameter estimation cannot be addressed without considering uncertainty, and the estimated parameter values are not fully useful without reporting the associated confidence interval, the procedure reported here was optimised using sensitivity and uncertainty analyses, both of which provided considerable insight into the problem by enabling an assessment of the quality and robustness of the resulting heat transfer correlations. The procedure was validated through its application to both synthetic and experimental data acquired from a TTHE for treating highly viscous fluid food.

2. Heat exchanger model

In this study, a TTHE operating in a counter-flow arrangement was considered, where the process fluid to be heated (e.g. sterilisation of a food fluid) flows into Section 2 (Figure 1), and the hot service fluid flows both in

Sections 1 and 3. The counter-flow configuration was chosen for this analysis because it is the most commonly adopted in industrial applications, since it provides the best performance.

The three fluids that passed through the system are assumed to be single-phase, incompressible with constant thermal properties. The inlet temperatures of the three fluids are assumed to be known, and so are the three mass flow rates (Figure 1b).

The heat exchanger is assumed to be in a steady-state regime and thermally insulated. Therefore, the heat transfer rates are obtained from the energy balance that for an infinitesimal fluid element is as follows:

$$dQ_1 = -\dot{m}_1 c_{p1} dT_1 \tag{1}$$

$$dQ_2 = -\dot{m}_2 c_{p2} dT_2 \tag{2}$$

$$dQ_3 = -\dot{m}_3 c_{p3} dT_3, \tag{3}$$

where $\dot{m}$ is the mass flow rate, c_p is the fluid specific heat at a constant pressure, and T is the fluid bulk temperature. The subscripts $_{1,2,3}$ indicate the fluids flowing in the Sections 1, 2, and 3 (Figure 1), respectively.

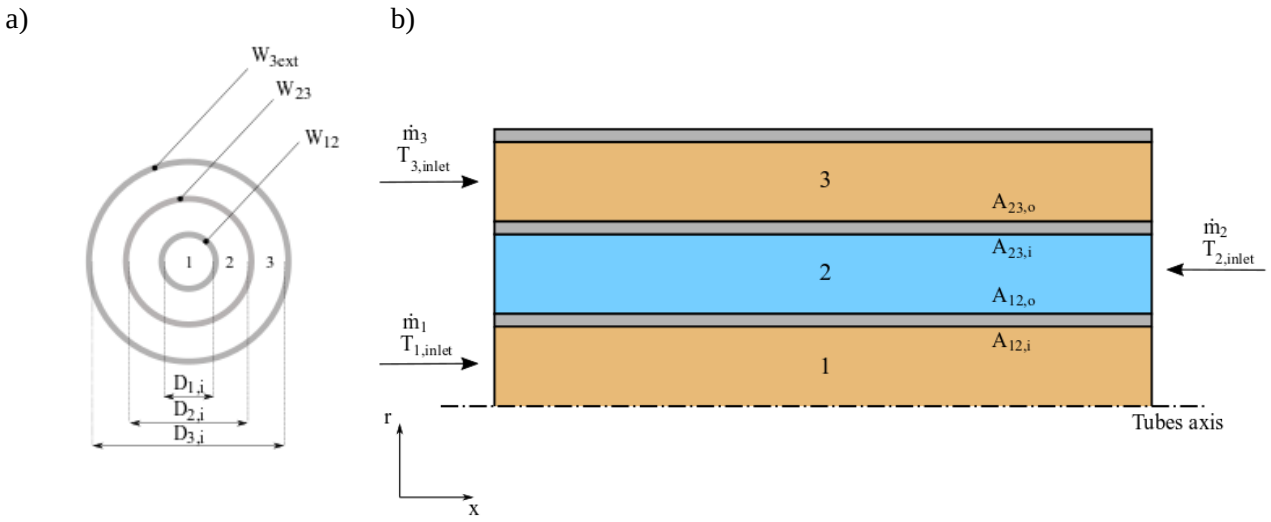

Figure 1. Schematic representation of the studied TTHE: (a) cross and (b) axial view.

The negative sign in the energy equations is due to the *x*-axis direction (Eq. (2)) and to the counter-current flows configuration (Eqs. (1,3)). Being the heat exchanger thermally insulated, the energy balance equation for the Section 2 (product side) can be evaluated also by:

$$dQ_2 = dQ_1 + dQ_3 \tag{4}$$

By introducing the overall heat transfer coefficients U_{12} between the product and the hot fluid that flows in Section 1 and U_{23} between the product and the hot fluid that flows in Section 3, Eqs. (1) and (3) can be rewritten as follows:

$$dQ_1 = U_{12} \Delta T_{12} dA_{12} \tag{5}$$

$$dQ_3 = U_{23} \Delta T_{23} dA_{23} \tag{6}$$

where:

- ΔT_{12} and ΔT_{23} are the temperature difference between the product and the hot fluid that flows in Section 1 and between the product and the hot fluid that flows in Section 3 for each axial coordinate, respectively:

$$\Delta T_{12} = T_1 - T_2 \tag{7}$$

$$\Delta T_{23} = T_3 - T_2 \tag{8}$$

- dA_{12} and dA_{23} are the heat transfer areas between Sections 1 and 2 and between Sections 2 and 3, respectively. They can be expressed in terms of the perimeter of the pipes, i.e. $dA = Pdx$. Therefore, Eqs. (5) and (6) can be rewritten as follows:

$$dQ_1 = U_{12}P_{12}\Delta T_{12}dx \tag{9}$$

$$dQ_3 = U_{23}P_{23}\Delta T_{23}dx \tag{10}$$

By substituting Eqs. (9) and (10) in Eq. (4):

$$dQ_2 = U_{12}P_{12}\Delta T_{12}dx + U_{23}P_{23}\Delta T_{23}dx \tag{11}$$

Therefore, the complete set of energy Equations (1–3) becomes:

$$\dot{m}_2 c_{p2} dT_2 = -U_{12}P_{12}\Delta T_{12}dx - U_{23}P_{23}\Delta T_{23}dx \tag{12}$$

$$\dot{m}_1 c_{p1} dT_1 = -U_{12}P_{12}\Delta T_{12}dx \tag{13}$$

$$\dot{m}_3 c_{p3} dT_3 = -U_{23}P_{23}\Delta T_{23}dx \tag{14}$$

Energy equations are solved by applying the finite difference method. Referring to Figure 2, Eqs. (12–14) can be reformulated as follows:

$$\dot{m}_2 c_{p2}\left(T_{2\,(k-1)} - T_{2\,(k)}\right) = U_{12}P_{12}(T_1 - T_2)_{(k)}\Delta x + U_{23}P_{23}(T_3 - T_2)_{(k)}\Delta x \tag{15}$$

$$\dot{m}_1 c_{p1}\left(T_{1\,(k)} - T_{1\,(k-1)}\right) = -U_{12}P_{12}(T_1 - T_2)_{(k-1)}\Delta x \tag{16}$$

$$\dot{m}_3 c_{p3}\left(T_{3\,(k)} - T_{3\,(k-1)}\right) = -U_{23}P_{23}(T_3 - T_2)_{(k-1)}\Delta x \tag{17}$$

where $k = 1,\ldots,K$ corresponds to the different axial coordinates at which the equations are solved, and Δx is the space step.

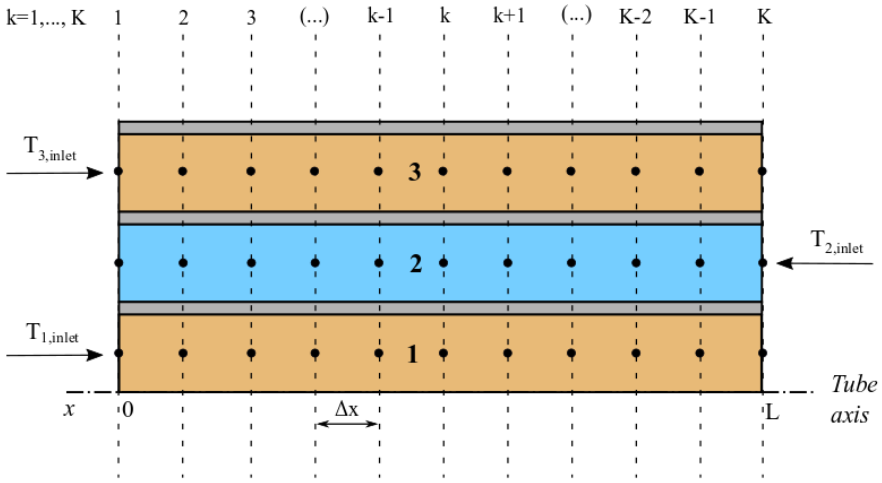

Figure 2. Finite difference **s**cheme of the investigated heat exchanger

Equations (15–17) are solved by considering the following boundary conditions:

$$\mathrm{T}_{2\,(K)} = \mathrm{T}_{2,inlet} \tag{18}$$

$$\mathrm{T}_{1\,(1)} = \mathrm{T}_{1,inlet} \tag{19}$$

$$\mathrm{T}_{3\,(1)} = \mathrm{T}_{3,inlet} \tag{20}$$

Therefore, the temperatures at the different *k* axial coordinates can be evaluated as follows:

$$\mathrm{T}_{2\,(k-1)} = \mathrm{T}_{2\,(k)} + \frac{\Delta x}{\dot{m}_2 \mathrm{c}_{p2}}\left[U_{21}P_{21}\left(\mathrm{T}_{1\,(k)} - \mathrm{T}_{2\,(k)}\right) + U_{23}P_{23}\left(\mathrm{T}_{3\,(k)} - \mathrm{T}_{2\,(k)}\right)\right] \tag{21}$$

$$\mathrm{T}_{1\,(k)} = \mathrm{T}_{1\,(k-1)} - \frac{U_{21}P_{21}\left(\mathrm{T}_{1\,(k-1)} - \mathrm{T}_{2\,(k-1)}\right)\Delta x}{\dot{m}_1 \mathrm{c}_{p1}} \tag{22}$$

$$\mathrm{T}_{3\,(k)} = \mathrm{T}_{3\,(k-1)} - \frac{U_{23}P_{23}\left(\mathrm{T}_{3\,(k-1)} - \mathrm{T}_{2\,(k-1)}\right)\Delta x}{\dot{m}_3 \mathrm{c}_{p3}} \tag{23}$$

The overall heat transfer coefficients *U* can be computed as [19]:

$$\frac{1}{U_{12i}A_{12i}} = \frac{1}{h_{12i}A_{12i}} + R_{w12} + \frac{1}{h_{12o}A_{12o}} \tag{24}$$

$$\frac{1}{U_{23i}A_{23i}} = \frac{1}{h_{23i}A_{23i}} + R_{w23} + \frac{1}{h_{23o}A_{23o}} \tag{25}$$

where A_{12i} and A_{12o} (Figure 1) are the internal and external heat transfer areas of Section 1, respectively, while A_{23i} and A_{23o} (Figure 1) are the internal and external heat transfer areas of Section 2, respectively; U_{12i} is the internal overall heat transfer coefficient between Sections 1 and 2; h_{12i} and h_{12o} are the internal and external convective heat transfer coefficients between Sections 1 and 2, respectively; U_{23i} is the internal overall heat transfer coefficient between Sections 2 and 3; h_{23i} and h_{23o} are the internal and external convective heat transfer coefficients between Sections 2 and 3, respectively. R_{w12} and R_{w23} are the wall thermal resistances, which can be computed as [23]:

$$R_{w12} = \frac{\ln[(D_{1o})/D_{1i}]}{2\pi\lambda_w L} \tag{26}$$

$$R_{w23} = \frac{\ln[(D_{2o})/D_{2i}]}{2\pi\lambda_w L} \tag{27}$$

where D_{1i} and D_{1o} are the internal and external diameters of Section 1, while D_{2i} and D_{2o} are the internal and external diameters of Section 2 (Figure 1), respectively; λ_w and L are the wall thermal conductivity and pipe length, respectively.

The convective heat transfer coefficients can be evaluated by Nusselt numbers, which are expressed by the following equations:

$$\mathrm{Nu}_1 = \frac{h_1 D_{1i}}{\lambda_1} \tag{28}$$

$$\mathrm{Nu}_2 = \frac{h_2 D_{2h}}{\lambda_2} \tag{29}$$

$$\mathrm{Nu}_3 = \frac{h_3 D_{3h}}{\lambda_3} \tag{30}$$

where D_{2h} and D_{3h} are the hydraulic diameters of Sections 2 and 3, respectively. The value of the Nusselt number can be computed if any correlation is already available in the literature or can be determined by conducting a set of experimental results as it is proposed in this study.
The Nusselt number in the fully developed region can be generally expressed as a function of Reynolds and Prandtl numbers [23]:

$$\mathrm{Nu}_1 = C_1 Re^{\alpha_1} Pr^{\beta_1} \tag{31a}$$

$$\mathrm{Nu}_2 = C_2 Re^{\alpha_2} Pr^{\beta_2} \tag{31b}$$

$$\mathrm{Nu}_3 = C_3 Re^{\alpha_3} Pr^{\beta_3} \tag{31c}$$

where C, α, β are a set of characteristic coefficients of each of the three sections of the heat exchanger under test. Hence, substituting in Eqs. (21–23) the definitions of U_{12i} and U_{23i} (Eqs. (24, 25)), where R_{w12} and R_{w23} are defined by Eqs. (26, 27) and h_1, h_2, h_3 are obtained from Eqs. (28–30) adopting the Nusselt number formulations given by Eqs. (31a–31c), it is possible to obtain:

$$\mathrm{T}_{2\,(k-1)} = \mathrm{T}_{2\,(k)} + \frac{\Delta x}{\dot{m}_2 c_{p2}}\left[\frac{1}{A_{12i}}\left(\frac{D_{1i}}{C_1 Re^{\alpha_1} Pr^{\beta_1}\lambda_1 A_{12i}} + R_{w12} + \frac{D_{2h}}{C_2 Re^{\alpha_2} Pr^{\beta_2}\lambda_2 A_{12o}}\right)^{-1} P_{21}\left(\mathrm{T}_{1\,(k)} - \mathrm{T}_{2\,(k)}\right) + \frac{1}{A_{23i}}\left(\frac{D_{2h}}{C_2 Re^{\alpha_2} Pr^{\beta_2}\lambda_2 A_{23i}} + R_{w23} + \frac{D_{3h}}{C_3 Re^{\alpha_3} Pr^{\beta_3}\lambda_3 A_{23o}}\right)^{-1} \cdot P_{23}\left(\mathrm{T}_{3\,(k)} - \mathrm{T}_{2\,(k)}\right)\right] \tag{32}$$

$$\mathrm{T}_{1\,(k)} = \mathrm{T}_{1\,(k-1)} - \frac{\frac{1}{A_{12i}}\left(\frac{D_{1i}}{C_1 Re^{\alpha_1} Pr^{\beta_1}\lambda_1 A_{12i}} + R_{w12} + \frac{D_{2h}}{C_2 Re^{\alpha_2} Pr^{\beta_2}\lambda_2 A_{12o}}\right)^{-1} P_{21}\left(\mathrm{T}_{1\,(k-1)} - \mathrm{T}_{2\,(k-1)}\right)\Delta x}{\dot{m}_1 c_{p1}} \tag{33}$$

$$\mathrm{T}_{3\,(k)} = \mathrm{T}_{3\,(k-1)} - \frac{\frac{1}{A_{23i}}\left(\frac{D_{2h}}{C_2 Re^{\alpha_2} Pr^{\beta_2}\lambda_2 A_{23i}} + R_{w23} + \frac{D_{3h}}{C_3 Re^{\alpha_3} Pr^{\beta_3}\lambda_3 A_{23o}}\right)^{-1} P_{23}\left(\mathrm{T}_{3\,(k-1)} - \mathrm{T}_{2\,(k-1)}\right)\Delta x}{\dot{m}_3 c_{p3}} \tag{34}$$

Eqs. (32–34) represent the direct formulation of the problem under study that is concerned with the determination of the outlet temperatures of the three sections when all the coefficients C, α, β are known. In the inverse formulation, the coefficients C, α, β are instead regarded as being unknown, whereas the outlet temperatures of the three sections are measured.

3. Parameter estimation and sensitivity analysis for characterising TTHE behaviour

The parameter estimation procedure is embedded in the inverse solution of the problem expressed by Eqs (32–34). The outlet temperatures of the three Sections T_1, T_2, and T_3 can be easily computed by imposing trial values of the coefficients C, α, β. In the inverse formulation, the computed values of the outlet temperatures are forced to match the experimental temperature values by tuning the coefficients C, α, β. The matching of the two temperature distributions (the computed and the experimentally acquired) could be easily performed using the least square approach. Therefore, the coefficients C, α, β could be estimated by minimising the following functional:

$$S(\boldsymbol{P}) = \sum_{n=1}^{N}\left[\boldsymbol{T}_{exp,n} - \boldsymbol{T}_{calc,n}\right]^2 \tag{35}$$

where $\boldsymbol{P}$ is the vector of the parameters that we want to estimate, $\boldsymbol{T}_{exp}$ and $\boldsymbol{T}_{calc}$ are the experimental and predicted variables, respectively, and N is the total number of measurements.

In a TTHE heat exchanger, the coefficients C, α, β must be estimated for all three sections in which the fluids are flowing: in this way, the number of unknowns ($\boldsymbol{P}$ vector) that must be found are 9. In the parameter estimation procedure adopted here, these 9 parameters are forced to vary using a nonlinear fit algorithm that is based on the iterative reweighted least squares method [24] to minimise the objective function expressed in Eq. (35). Being a nonlinear regression, it requires a significant computational cost and an elevated number of measurements to properly estimate all the unknowns. Hence, when discussing parameter estimation procedures and inverse problems in general, it is fundamental to do all the simplifications that can be reasonably performed. In the present case, we can make the following simplifications:

- The β coefficients that characterise the dependency of the Nusselt number on the Prandtl number can be considered to be 0.4 in heating processes and 0.3 in cooling processes. This choice is very common, even when DTHEs are considered, because β coefficients have a limited impact on the accuracy of the Nusselt correlation.
- C and α for the Section 1 can be found from one of the correlations available in the literature for straight smooth wall tube. This geometric configuration has been widely studied in the past, and considering that most times, the fluid flowing in section 1 is in turbulent regime, it is a reasonable approximation to consider them a priori known.
- The same argumentation for Section 1 could also be done for Section 3: in this case, we are talking about an annular section that has been deeply investigated in literature too.

After these considerations, the number of unknowns is decreased to two: C and α for Section 2, that we are going to call in the following C_2 and α_2.

To endorse the assumptions explained above, from the practical viewpoint, these two parameters are the crucial ones in the design process in the great majority of applications of TTHE because these heat exchangers are especially adopted for highly viscous fluids and, consequently, the thermal resistance of the product side is dominant in the overall heat exchange performance.

Finally, the function that should be minimised using the usual least squares approach can be written as follows:

$$S(C_2, \alpha_2) = \sum_{i=1}^{M} \left[\boldsymbol{T}_{exp,i} - \boldsymbol{T}_{calc,i} \right]^2 \tag{36}$$

where $\boldsymbol{T}_{exp}$ is the measurement vector composed as follows:

$$\boldsymbol{T}_{exp} = [T_{1,outlet}, T_{2,outlet}, T_{3,outlet}] \tag{37}$$

$T_{1,outlet}$, $T_{2,outlet}$, and $T_{3,outlet}$ are the outlet temperatures of the three sections measured for the N tests. Consequently, the vector $\boldsymbol{T}_{exp}$ has dimensions $1 \times M$ where $M = 3 \cdot N$. Analogously, it works for the vector $\boldsymbol{T}_{calc}$ obtained by solving the direct problem described by Eqs (32–34) by imposing the values of the coefficients C, α, β.

Then, the parameter estimation procedure applied to the heat transfer characterisation of TTHE results in the minimisation of the objective function S given by Eq. (36) by assuming Re and Pr as the independent variables, C_2 and α_2 as the unknown variables, and all the other properties and geometrical quantities as known.

The practical possibility of concurrently estimating all the unknown parameters (C_2 and α_2) is feasible only if the parameter sensitivity coefficients for the output variable T with respect to each parameter are linearly independent over the range of interest [23]. In practice, the sensitivity coefficients quantify the extent to which variations in the parameters of interest affect the answer output of the system. The coefficients are then defined with respect to the generic parameter P_i as follows:

$$J_i = \frac{\partial \boldsymbol{T}}{\partial P_i} P_i \tag{38}$$

where P_i stands for the unknown variables, i.e. C_2 and α_2, and $\boldsymbol{T}$ is the outlet temperature vector (Eq.37).

Although sensitivity analysis is a useful tool to theoretically verify the possibility of concurrently estimating several unknown variables, it lacks quantitative information about the uncertainty associated with each estimated value [17]. A well-known method used to address this issue involves the computation of confidence intervals for parameter estimates by asymptotic theory [25, 26]. Following this approach, once the optimal curve-fit parameters P_{fit} are determined, the parameter standard errors σ_P are given by:

$$\boldsymbol{\sigma}_P = \sqrt{\sigma_T^2 \cdot diag([\boldsymbol{J}^T \cdot \boldsymbol{J}]^{-1})} \tag{39}$$

where $\boldsymbol{J}$ is the Jacobian matrix of the target variable, i.e. the function $\boldsymbol{T}_{calc}$:

$$\boldsymbol{J} = \left[\frac{\partial \boldsymbol{T}_{calc}(\boldsymbol{P}_{fit})}{\partial \boldsymbol{P}}\right] \tag{40}$$

and σ^2_T is the residual variance:

$$\sigma_T^2 = \frac{1}{M - z}\sum_{i=1}^{M}\left[\boldsymbol{T}_{exp,i} - \boldsymbol{T}_{calc,i}(\boldsymbol{P}_{fit})\right] \tag{41}$$

where M is the number of measurements, and z is the number of parameters to be fitted.

To express the reliability of the parameter estimates and to compare the relative precision of different parameter estimates, the 95% confidence interval, $CI^{95\%}$, and the coefficient of variation, CV, are generally used [25]. Regarding the parameter P_i, they are defined as follows:

$$CI_{P_i}^{95\%} = (P_i - 1.96\sigma_{P_i}, P_i + 1.96\sigma_{P_i}) \tag{42}$$

$$CV_{P_i} = \frac{\sigma_{P_i}}{P_i} \tag{43}$$

4. Application of the parameter estimation procedure to synthetic data

Before the experimental measurements were used, the parameter estimation procedure was validated using synthetic data. The geometrical and thermal characteristics of the TTHE and the inlet temperature of the product and service fluids are summarised in Table 1. These geometrical characteristics were chosen because the proposed method was validated against the experimental data obtained using this type of heat exchanger. These properties and the proper Nusselt number correlations, both for the pipe and shell sides, allow the evaluation of the heat transfer mechanism.

Table 1. Geometrical and setup characteristics of the TTHE

D_{1i} (mm)	D_{1o} (mm)	D_{2i} (mm)	D_{2o} (mm)	D_{3i} (mm)	D_{3o} (mm)	L (m)	W_{12} (mm)	W_{23} (mm)	A_{12i} (m^2)
40.9	48.3	66.9	73.0	83.8	88.9	10.1	3.7	3.1	1.3

A_{12o} (m^2)	A_{23i} (m^2)	A_{23o} (m^2)	λ (W/m·K)	$T_{1,inlet}$ (°C)	$T_{2,inlet}$ (°C)	$T_{3,inlet}$ (°C)
1.5	2.1	2.3	15	120	50	120

Synthetic data for the outlet temperatures of the three sections were obtained by solving the direct problem described by Eqs (32–34) by imposing the values of the coefficients C, α, β.

It was considered a possible application in the food industry: water is assumed as service heating fluid that flows in Sections 1 and 3, while a highly viscous product flows (i.e. fruit purees or concentrated juices) in Section 2 in a counter-current configuration. Constant physical properties are considered: $\rho_S = 1000$ Kg·m^{-3}, $\mu_S = 10^{-3}$ Pa·s, and $\lambda_S = 0.6$ W·m^{-1}·K^{-1} for the water, while the product is characterised by $\rho_P = 1054$ kg·m^{-3}, $\mu_P = 2.6\cdot10^{-1}$ Pa·s, and $\lambda_P = 5.9\cdot10^{-1}$ W·m^{-1}·K^{-1}, calculated considering a 16°Bx juice at 50°C [27].

The fluids flowing in Sections 1 and 3 were considered flowing in turbulent regime: Re_1 and Re_3 were kept fixed at $2.1\cdot10^5$, while the product was considered in a laminar condition with Re_2 varying in the range of 5–500, generating a set of 100 tests. Synthetic noiseless data are obtained with Eqs. (32–34) assuming $C_1 = C_2 = C_3 = 0.023$, $\alpha_1 = \alpha_2 = \alpha_3 = 0.8$, $\beta_1 = \beta_3 = 0.3$, and $\beta_2 = 0.4$.

To simulate the presence of experimental noise, the synthetic data obtained from the solution of the direct problem (Eqs (32–34)), were deliberately spoiled by random noise. A Gaussian white noise was introduced. The *T* synthetic data were generated according to the following:

$$\begin{aligned} T_{1,outlet} &= T_{1,outlet,noiseless} + \zeta\epsilon \\ T_{2,outlet} &= T_{2,outlet,noiseless} + \zeta\epsilon \\ T_{3,outlet} &= T_{3,outlet,noiseless} + \zeta\epsilon \\ T_{1,inlet} &= T_{1,inlet,noiseless} + \zeta\epsilon \\ T_{2,inlet} &= T_{2,inlet,noiseless} + \zeta\epsilon \\ T_{3,inlet} &= T_{3,inlet,noiseless} + \zeta\epsilon \end{aligned} \tag{44}$$

where ζ is the temperature noise level, and ϵ is a random Gaussian variable with zero mean and unit variance. Five different noisy datasets were generated using five levels of noise, specifically, ζ = 0.01 K, ζ = 0.05 K, ζ= 0.1 K, ζ = 0.5 K, and ζ = 1 K. Finally, the noisy datasets were elaborated with the inverse estimation procedure based on the minimisation of the squared errors of the prediction with respect to the experimentally measured outlet temperatures values (Eq. (36)).

The objective of this procedure is to find a correlation for the Nusselt number that can describe the heat transfer behaviour of Section 2 of the heat exchanger. To reach this goal and refer to Eq. (31), it is necessary to estimate, as highlighted in paragraph 3, the coefficients *C* and α for Section 2.

To verify the practical possibility of concurrently estimating the two parameters (C_2 and α_2), it is important to analyse the behaviour and the relative magnitude of their sensitivity coefficients versus the independent variables, i.e. the Reynolds number in Section 2. The sensitivity coefficients calculated regarding the vector composed of the outlet temperatures of the three sections (Eq. (37)) of the heat exchanger were reported in Figure 3.

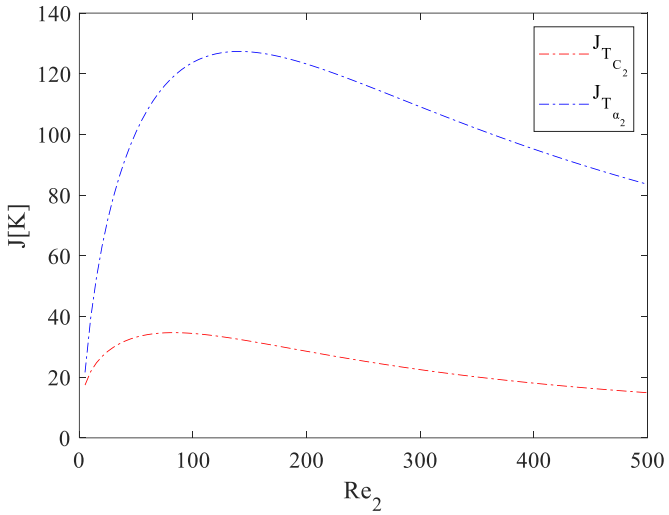

Figure 3. Sensitivity coefficients versus the Reynolds number

Figure 3 shows that $J_{T_{c_2}}$ displays a linear independence from $J_{T_{\alpha_2}}$ for Re_2 lower than 400, while for higher values, they are not completely linearly independent. The highest values of sensitivity coefficients are obtained in the range 50 < Re_2 < 300 for $J_{T_{c_2}}$ and in the range 100 < Re_2 < 350 for $J_{T_{\alpha_2}}$. This evidence means that the optimal estimation of both C_2 and α_2 can be obtained for product Reynolds number values between 100 and 300 and that their concurrent estimation in the same Reynolds number range is feasible since they are linearly independent. The fact that the highest sensitivity coefficients can be found for Re_2 lower than 300 is related to the elevated values that the thermal resistance of the product side assumes when the mass product flow is low: being the flow in Sections 1 and 3 turbulent (i.e. low value of thermal resistance) the greatest contribution to overall thermal resistance of the heat exchanger is due to the one related to Section 2, permitting to have a high sensitivity in the estimation of the coefficients that describe the thermal behaviour of that section. Another

important element is related to the fact that the sensitivity coefficient for α_2 presents significantly higher values than that for C_2, highlighting that its estimation can be performed with higher accuracy.

To better investigate this point, the influence of the estimated parameters on the overall heat transfer coefficients was evaluated. In Figure 4, the sensitivity coefficients for U_{12} and U_{23} as a function of the Reynolds number of the product are presented.

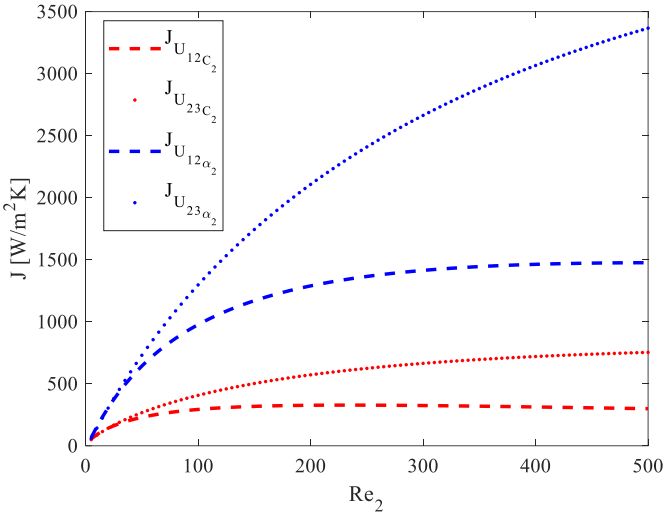

Figure 4. Sensitivity coefficients versus the Reynolds number

The sensitivity coefficient for α_2 presented significantly higher values than that for C_2, confirming that the estimation of α_2 could be performed with higher accuracy, as also highlighted above by the sensitivity coefficient for the outlet temperatures.

The uncertainty associated with each estimated parameter value was assessed using the parameter covariance matrix by asymptotic theory [25, 26]. Both the 95% confidence intervals and the coefficients of variation are calculated according to Eqs. (42, 43).

Table 2 reports the results of the minimisation for each level of noise, and in Figure 5, they are graphically shown as the trend of the coefficients of variation as a function of noise level. It is possible to observe that the adopted estimation procedure helps to obtain a great estimation of the unknown coefficients.

Table 2. Results of parameter estimation with synthetic data

Noise level (ζ)	Unknown parameter	exact value	estimated value	CI $^{95\%}$	CV (%)
0.01	C_2	0.023	0.023	(0.023, 0.023)	0.04%
	α_2	0.800	0.800	(0.800, 0.800)	0.01%
0.05	C_2	0.023	0.023	(0.023, 0.023)	0.23%
	α_2	0.800	0.800	(0.799, 0.801)	0.06%
0.1	C_2	0.023	0.023	(0.023, 0.023)	0.45%
	α_2	0.800	0.800	(0.796, 0.801)	0.12%
0.5	C_2	0.023	0.023	(0.022, 0.024)	2.03%
	α_2	0.800	0.803	(0.794, 0.811)	0.52%
1	C_2	0.023	0.023	(0.021, 0.025)	4.2%
	α_2	0.800	0.802	(0.785, 0.819)	1.07%

Even for the highest noise level (ζ = 1 K), the confidence intervals and the CVs, for both C_2 and α_2, are very small, confirming the efficacy of the estimation procedure. In the worst conditions, the highest value of CV is 4.2%, underlying the excellent results achieved. Moreover, the higher values of CV for C_2 with respect to those

of α_2 confirm what can be seen from the sensitivity coefficients reported in Fig. 3, where $J_{T_{C_2}}$ displays lower values than $J_{T_{\alpha_2}}$, revealing—even if slightly—a major difficulty in the estimation of C_2.

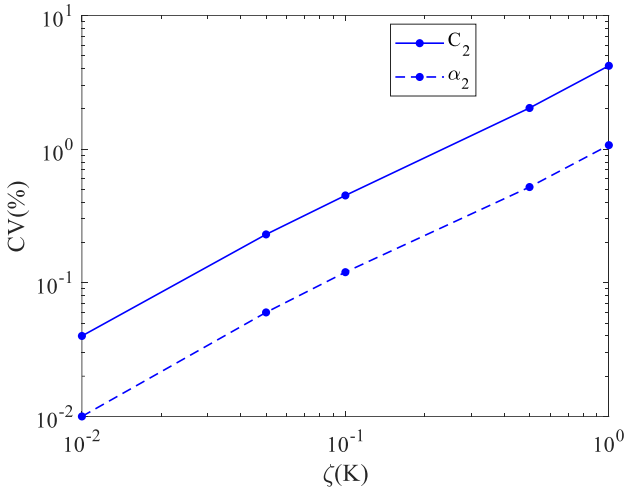

Figure 5. Coefficients of variation obtained with synthetic data for different noise levels

To give additional insight in evaluating the effectiveness of the proposed estimation approach at different noise level values, a residual analysis was conducted by computing the relative estimation error on the heat power exchanged by the product Q_2, defined as follows:

$$E_{Q_2} = \frac{\|(\boldsymbol{Q_2})_{estimated} - (\boldsymbol{Q_2})_{exact}\|_2}{\|(\boldsymbol{Q_2})_{exact}\|_2} \tag{45}$$

where $(\boldsymbol{Q_2})_{estimated}$ and $(\boldsymbol{Q_2})_{exact}$ are the vectors composed by the restored and exact heat power values of the 100 considered tests. This estimation error is calculated on the heat power exchanged by product since it is the quantity of major interest in heat exchangers: the final goal is that the product receives or dissipates the prescribed heat power. The E_{Q_2} distribution as a function of the noise is reported in Figure 6a, while, in Figure 6b, it is shown as the deviation of the computed values of Q_2 obtained using the estimated parameters with respect to the exact values regarding the highest noise level (ζ = 1 K).

a) b)

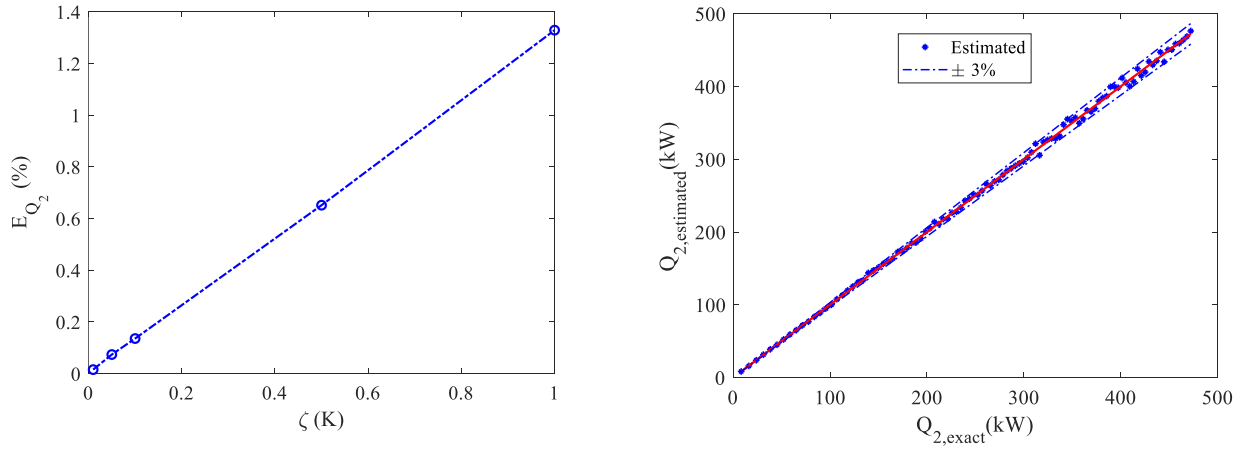

Figure 6. Estimation error E_{Q_2} as a function of the noise level (a) and comparison between exact and estimated heat power Q_2 for noise level ζ = 1 K (b)

The estimation error (Fig. 6a) on the exchanged heat power underlines the high efficacy of the present procedure, showing very low values with a maximum of 1.4%. Moreover, the random distribution of the estimated heat power values respect to the exact ones emphasises the high assessment ability of the proposed method: all the values (Fig. 6b) are within a ±3% band.

5. Application of the parameter estimation approach to experimental data

5.1 Experimental facility

The estimation methodology described above is assessed in a TTHE located in the pilot plant of the company JBT-FoodTech (Parma–Italy). The heat exchanger, made of AISI 304 and characterised by the geometrical features reported in Table 1, is schematically represented in section in Fig. 7(a) and in 3D view in Fig. 7(b).

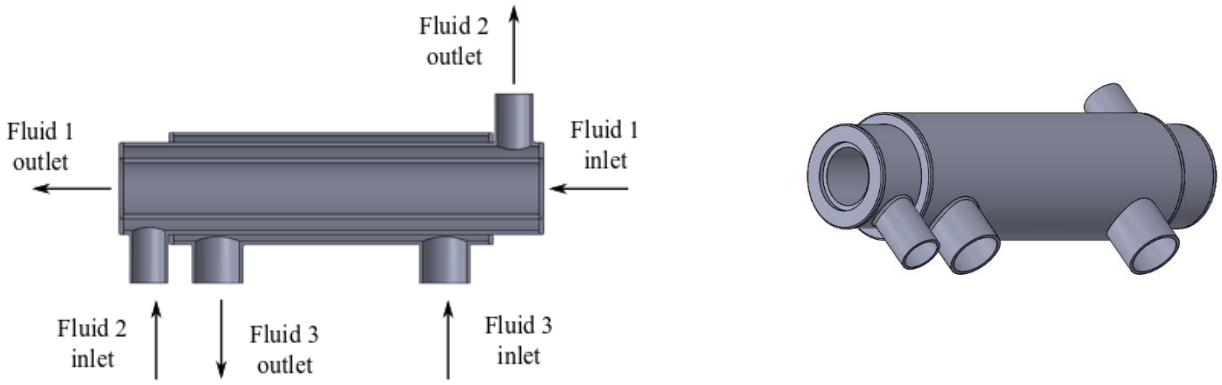

Figure 7. (a) Sketch of the section of the experimentally tested THE and (b) 3D view

The scheme of the experimental setup where the tested TTHE is inserted is shown in Figure 8. It essentially comprises a hydraulic circuit coupled with a data acquisition system. The hydraulic circuit moves the treated fluid (tomato double concentrate), which is heated through the TTHE, then it passes to a short thermal rest section, and finally is cooled, so that it can be used again under the same initial conditions.

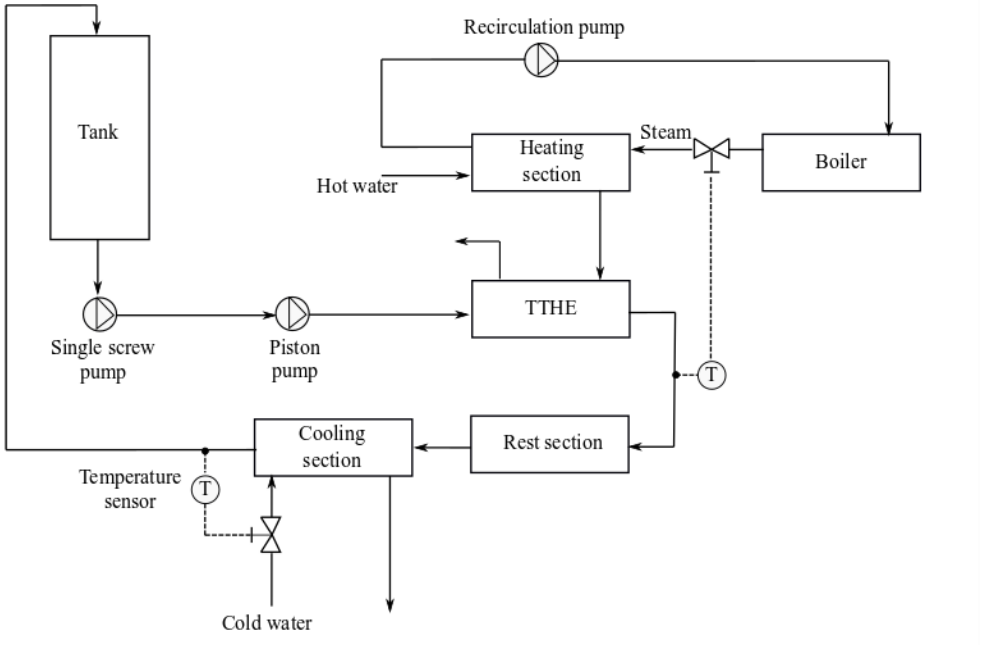

Figure 8. Scheme of the experimental setup

The product is loaded into a feed tank with a capacity of about 0.5 m^3 and supported by a single screw volumetric feed pump that sends the product into a piston pump controlled by a frequency variator. The service fluid used to heat the product is hot water heated using a tube-in-tube heat exchanger, in which steam produced by an external boiler circulates. The steam flow rate is controlled in feedback from the product outlet temperature of the TTHE through a modulating valve. For the cooling of the product, a series of dimpled tube exchangers are used in which cold water circulates. The flow rate of cold water is controlled in feedback from the outlet temperature of the product in the cooling section. Finally, to prevent heat transfer with the external environment, the heat exchanger was thermally insulated all lengths long of its transfer area.

The product flow rate is measured using a Rosemount electromagnetic flowmeter placed between the piston pump and the TTHE. The hot water flow rate is measured using a Siemens electromagnetic flowmeter positioned before the heating section. The measurement of the product inlet temperature in Section 2 is done by Pt 100 thermo-resistances placed inside the feed tank. The product outlet temperature is measured with another thermo-resistance placed at the end of Section 2. For the hot water that flows in Sections 1 and 3, four thermo-resistances measured the temperature at the inlet and at the outlet of both Sections 1 and 3.

In the data reduction, the average bulk temperature between the inlet and outlet sections is used for evaluating all fluids properties. For the fluids' properties, the tabulated values reported by [23] was used. However, the tested product is double tomato concentrate, and the definition of its properties can be quite tricky; particularly, the determination of viscosity is critical due to its non-Newtonian behaviour.

The viscosity μ_P of the double tomato concentrate for each test was determined according to the Ostwald-de Waele model [27]:

$$\mu_P = \frac{\tau_P}{\dot{\gamma}} = -\frac{K \cdot \dot{\gamma}^n}{\dot{\gamma}} = -K(\dot{\gamma})^{n-1} \tag{46}$$

where, K is the consistency index, $\dot{\gamma}$ is the shear rate, and n is the flow behaviour index.

A Brookfield R/S+ rheometer equipped with the coaxial cylinder probe CC25 in the 'Searle system' configuration is used to measure the shear stress (τ_b) of the tomato concentrate by varying the share rate in the range of 0.13–1290 s^{-1} at four different temperatures: 20°C, 30°C, 40°C, and 50°C. Values of K and n are determined as follow:

$$n = \frac{d(\ln \tau_P)}{d(\ln V_r)} \tag{47}$$

$$K = \frac{\exp i}{(\frac{\pi}{15\, n} \cdot \frac{1}{1 - (\frac{R_b}{R_c})^{2/n}})^n} \tag{48}$$

where V_r, R_b, and R_c are the rotation velocity of the internal cylinder, the radius of the cylinder, and the internal radius of the external cylinder, respectively. To reduce the number of viscosity tests according to Trifirò et al. [28], an exponential dependence on temperature for K value and a linear one for n value is assumed, and a regression is performed using these two models:

$$K = K_0 \cdot K_T^{(\frac{1000}{T})} \tag{49}$$

$$n = n_0 + n_T \cdot 1000/T \tag{50}$$

where K_0, K_T, n_0, and n_T are the parameters to determine and calculate the values of n and K for any value of temperature of interest in the range considered for the tests using Eq. (46).

The generalised Reynolds number values were then calculated, adopting the equation given by Kozicki et al. [29], valid for non-Newtonian fluids flowing in an annular section:

$$Re_g = \frac{\rho\, \bar{u}^{2-n} D_h^n}{8^{n-1} K (b + \frac{a}{n})^n} \tag{51}$$

where D_h is the hydraulic diameter, and a and b are geometrical parameters considered equal to 0.499 and 0.999, respectively.

5.2 Results

To consider the typical operating conditions of TTHEs in the food industry, which generally handle highly viscous fluids, double tomato concentrate was used as the working fluid, and water was used as the service fluid. Table 3 reports the experimental conditions of the test runs. In the data processing and in the definition of the dimensionless parameters, the properties of the working fluid (double tomato concentrate) were evaluated at the average bulk temperature between the inlet and outlet sections.

Importantly, although the adopted working fluid is non-Newtonian and has a very high viscosity, the heat dissipation due to the fluid friction is negligible in the considered case. In particular, the dissipated heat was less than 1% of the exchanged heat for all the performed experimental tests.

Table 3. Experimental conditions

Test	$\dot{m}_2$	$T_{1,inlet}$	$T_{1,outlet}$	$T_{2,inlet}$	$T_{2,outlet}$	$T_{3,inlet}$	$T_{3,outlet}$	Re_1	Pr_1	Re_{g2}	Pr_{g2}	Re_3	Pr_3
1	5.70	56.5	53.5	21.9	50.1	56.5	55.4	$4.5{\cdot}10^3$	3.2	4.3	$6.2{\cdot}10^3$	$7.3{\cdot}10^4$	3.2
2	5.71	58.1	54.5	21.8	50.2	58.1	56.7	$4.0{\cdot}10^3$	3.1	5.7	$5.4{\cdot}10^3$	$7.8{\cdot}10^4$	3.1
3	5.71	59.2	55.3	22.2	50.3	59.2	57.6	$3.9{\cdot}10^3$	3.0	7.0	$5.0{\cdot}10^3$	$8.0{\cdot}10^4$	3.0
4	5.71	60.8	56.3	22.0	50.4	60.8	59	$4.2{\cdot}10^3$	3.0	8.7	$4.5{\cdot}10^3$	$8.1{\cdot}10^4$	3.0
5	5.71	60.9	55.9	21.8	50.2	60.9	58.8	$4.7{\cdot}10^3$	3.0	10.8	$4.1{\cdot}10^3$	$7.8{\cdot}10^4$	3.0
6	5.71	60.6	55.4	21.7	50.2	60.6	58.4	$4.6{\cdot}10^3$	3.0	12.6	$3.8{\cdot}10^3$	$7.9{\cdot}10^4$	3.0
7	5.70	60.2	54.7	21.7	50.2	60.2	57.8	$4.4{\cdot}10^3$	3.0	14.6	$3.6{\cdot}10^3$	$7.8{\cdot}10^4$	3.0
8	5.70	60.6	55	21.7	50.3	60.6	58.2	$5.0{\cdot}10^3$	3.0	15.7	$3.5{\cdot}10^3$	$7.6{\cdot}10^4$	3.0
9	5.71	61.2	55.3	21.7	50.2	61.2	58.6	$4.9{\cdot}10^3$	3.0	18.1	$3.3{\cdot}10^3$	$7.8{\cdot}10^4$	3.0
10	5.72	62.2	55.9	21.7	50.3	62.2	59.4	$4.6{\cdot}10^3$	3.0	20.4	$3.1{\cdot}10^3$	$8.0{\cdot}10^4$	3.0
11	5.71	61.9	55.5	22.3	50.2	61.9	59.0	$4.6{\cdot}10^3$	3.0	23.0	$3.0{\cdot}10^3$	$8.0{\cdot}10^4$	3.0
12	5.66	121.3	106.9	49.3	99.0	121.3	114.1	$8.7{\cdot}10^3$	1.5	51.1	$1.6{\cdot}10^3$	$16{\cdot}10^4$	1.5
13	5.66	120.9	107.0	48.2	98.3	120.9	114.1	$8.8{\cdot}10^3$	1.5	41.5	$1.7{\cdot}10^3$	$15{\cdot}10^4$	1.5
14	5.66	121.0	108.6	48.9	98.8	121.0	114.9	$8.5{\cdot}10^3$	1.5	33.1	$1.9{\cdot}10^3$	$16{\cdot}10^4$	1.5
15	5.67	115.0	104.8	49.5	98.5	115.0	110.1	$8.1{\cdot}10^3$	1.5	24.1	$2.2{\cdot}10^3$	$15{\cdot}10^4$	1.5
16	5.67	113.1	104.1	50.6	98.6	113.1	108.8	$8.1{\cdot}10^3$	1.6	19.2	$2.4{\cdot}10^3$	$15{\cdot}10^4$	1.6
17	5.67	113.1	104.6	49.5	98.4	113.1	109.1	$6.6{\cdot}10^3$	1.6	15.7	$2.6{\cdot}10^3$	$15{\cdot}10^4$	1.6
18	5.67	111.8	104.7	49.6	98.5	111.8	108.5	$6.6{\cdot}10^3$	1.6	9.7	$3.2{\cdot}10^3$	$15{\cdot}10^4$	1.6
19	5.67	105.6	101.0	49.1	98.4	105.6	103.7	$4.4{\cdot}10^3$	1.7	5.0	$4.3{\cdot}10^3$	$15{\cdot}10^4$	1.7

The measured and calculated values of the outlet temperatures of the three sections of the TTHE are forced to match by minimising the functional given by Eq. (36), as described in the previous paragraph.

The estimated values of C_2 and α_2 for the product side are reported in Table 4 with the confidence intervals and the coefficient of variation.

Table 4. Estimates values for the experimental data set

Unknown parameter	**Estimated value**	**CI$^{95\%}$**		**CV**
C_2	0.313	0.273	0.354	6.55%
α_2	0.707	0.662	0.751	3.20%

As predicted by applying the estimation procedure to the synthetic data, the highest uncertainty is associated with estimating the multiplicative constant C_2 (coefficient of variation of approximately 6.5%), while the Reynolds number exponent α_2 is determined with a coefficient of variation of approximately 3%. Anyway,

both the parameters have been estimated with a very small coefficient of variation and limited confidence intervals, demonstrating the goodness of the parameter estimation approach presented here.

The experimental values of heat power exchanged by the product Q_2 are compared in Figure 9 to the values obtained using the optimal correlation found for Section 2:

$$\mathrm{Nu}_2 = 0.313\, Re^{0.707} Pr^{0.4} \tag{52}$$

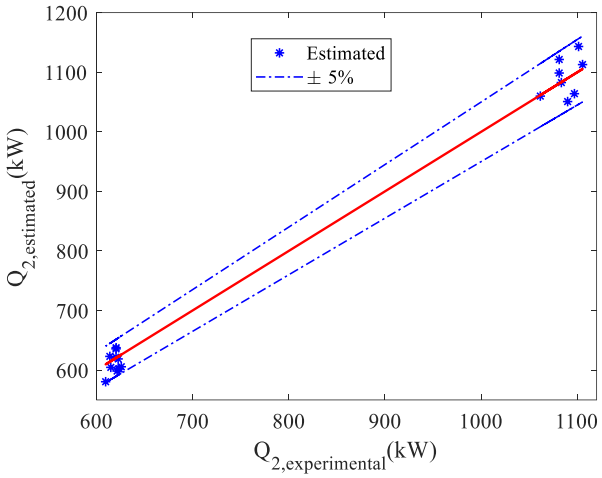

Figure 9. Comparison between experimental and estimated heat power Q_2

The results show that the correspondence between experimental and estimated heat power Q_2 is very good, proving that the correlation for the product Nusselt number is adequate: all the results are within a band of uncertainty of ± 5%. Moreover, the estimation error computed with Eq. (45) corresponds to 2.7%. It is not surprising that the global estimation error related to the correlation in Eq. (52) is smaller than the maximum uncertainty of the various coefficients and exponents (Table 4) because these terms are related to each other, and the simple propagation of error approach cannot be employed [30].

Finally, for the considered case, as far as the correspondence between experimental and estimated heat power is already excellent from an engineering viewpoint, the implementation of a more complicated model is not recommended because it would require a more extensive experimental campaign, giving negligible beneficial results.

6. Parameter estimation extension: 4 and 6 parameters

To further study the possibilities given by the described estimation method, two variants of the procedure defined in paragraph 4 are considered: estimation of 4 parameters (C_2, α_2, C_3, α_3) and estimation of 6 parameters (C_1, α_1, C_2, α_2, C_3, α_3). Then the functional to be minimised (Eq. (36)) becomes:

$$S(C_2, \alpha_2, C_3, \alpha_3) = \sum_{i=1}^{M} \left[\boldsymbol{T}_{exp,i} - \boldsymbol{T}_{calc,i} \right]^2 \tag{51a}$$

$$S(C_1, \alpha_1, C_2, \alpha_2, C_3, \alpha_3) = \sum_{i=1}^{M} \left[\boldsymbol{T}_{exp,i} - \boldsymbol{T}_{calc,i} \right]^2 \tag{51b}$$

For 4 parameters estimation, the choice of considering as known the coefficients of Section 1 and not those of Section 3 is because Section 1 is constituted by a straight smooth wall tube: this geometric configuration is the most investigated in the available literature and, thus, it will be easier to find the correlation that perfectly fits the conditions of the studied case with respect to Section 3, which is an annular section that is also a deeply investigated geometry but surely less than smooth straight tube.

Regarding 2-parameter case, Re_3 is not kept fixed but is assumed to vary in the range $10^4 < \mathrm{Re}_3 < 1.9 \cdot 10^4$ with the number of tests that is increased to 200.

In Table 5, they are reported the parameter values obtained from the minimisation together with 95% confidence intervals and the coefficients of variation for 4-parameter estimation. In Figure 10, to help the visualisation of the results, the trend of the coefficients of variation are graphically shown as a function of noise level.

Table 5. Results of parameter estimation on synthetic data (4 parameter case)

Noise level (ζ)	Unknown parameter	Exact value	Estimated value	CI 95%	CV (%)
0.01	C_2	0.023	0.023	(0.023, 0.023)	0.02%
	α_2	0.800	0.800	(0.800, 0.800)	0.01%
	C_3	0.023	0.023	(0.022, 0.024)	2.57%
	α_3	0.800	0.801	(0.796, 0.807)	0.33%
0.05	C_2	0.023	0.023	(0.023, 0.023)	0.11%
	α_2	0.800	0.800	(0.800, 0.801)	0.03%
	C_3	0.023	0.024	(0.018, 0.030)	13.63%
	α_3	0.800	0.796	(0.768, 0.824)	1.79%
0.1	C_2	0.023	0.023	(0.023, 0.023)	0.22%
	α_2	0.800	0.798	(0.800, 0.802)	0.06%
	C_3	0.023	0.028	(0.013, 0.043)	27.37%
	α_3	0.800	0.781	(0.725, 0.837)	3.65%
0.5	C_2	0.023	0.022	(0.022, 0.023)	1.08%
	α_2	0.800	0.808	(0.795, 0.804)	0.31%
	C_3	0.023	0.030	(-0.055, 0.116)	144.70%
	α_3	0.800	0.781	(0.485, 1.076)	19.32%
1	C_2	0.023	0.024	(0.022, 0.024)	2.17%
	α_2	0.800	0.790	(0.795, 0.814)	0.62%
	C_3	0.023	0.048	(-0.196, 0.292)	257.68%
	α_3	0.800	0.719	(0.193, 1.245)	37.32%

From Table 5 and Figure 10, the adopted procedure helps in obtaining a very good estimation of all the unknown parameters until a noise level of 0.1 K even if the confidence intervals of C_3 become larger and the coefficient of variation reach a maximum value of 27%.

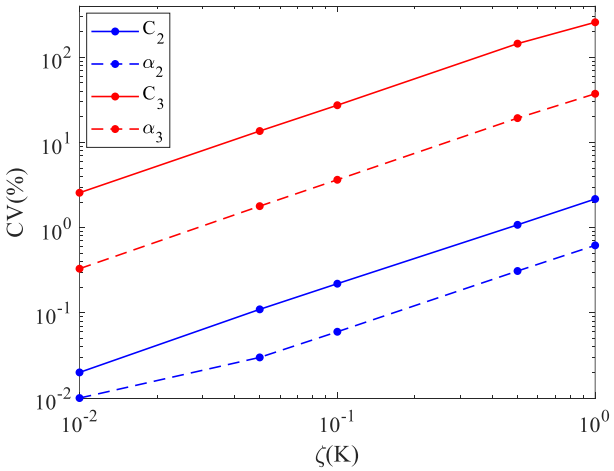

Figure 10. Coefficients of variation for different noise levels for 4-parameter estimation

For noise levels of 0.5 and 1 K, the parameter restoration is still satisfying for all the unknowns but the confidence of variance of C_3 rises significantly, and the one of α_3 increases to 19% and 37%, respectively. Concurrently, the confidence intervals greatly widen. Nevertheless, the estimation of C_2 and α_2 is still optimal for all the noise levels: CV values and confidence intervals of the product side coefficients are comparable to the ones obtained for the 2-parameter estimation. This behaviour occurs because, in the usual TTHE working conditions, the most part of the thermal resistance is due to the contribution of the product side: consequently, it is easier to estimate the coefficients that describe the behaviour of Section 2 with respect to the ones of Section 3, whose variation does not significantly affect the overall thermal resistance.

in Figure 11a, it is reported as the estimation error on the heat power exchanged by the product (Eq. (45)), while in Figure 11b, it is shown as the comparison between the computed values of Q_2 and the exact ones regarding the highest noise level (ζ = 1 K).

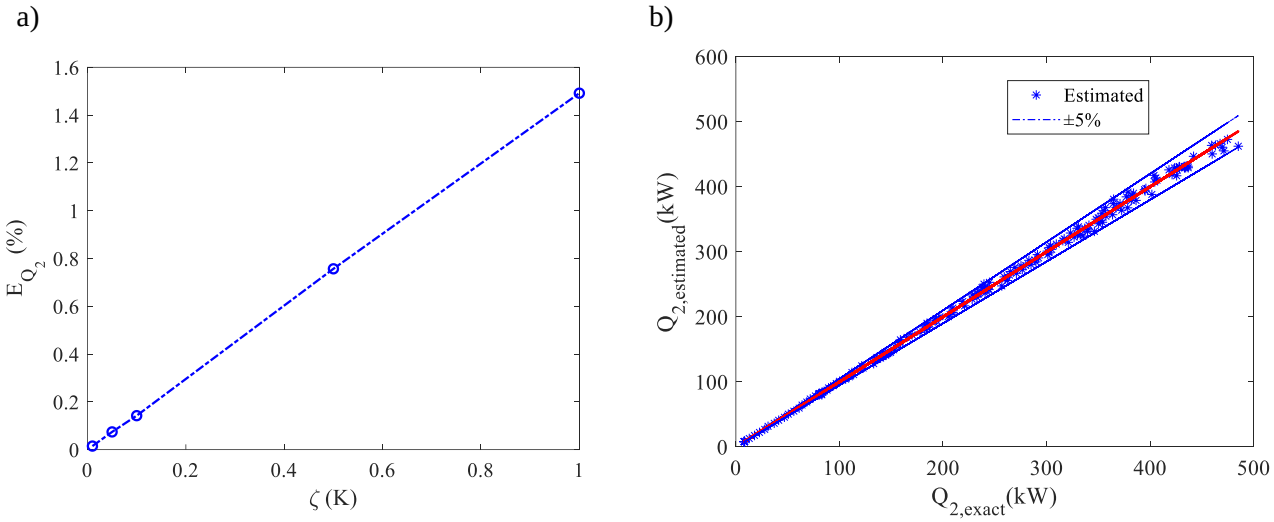

Figure 11. Estimation error E_{Q_2} as a function of the noise level (a) and comparison between exact and estimated heat power Q_2 for noise level ζ = 1 K (b) for 4-parameter estimation

As in 2-parameter estimation, the estimation error (Fig. 11a) on the exchanged heat power Q_2 is characterised by very small values with a maximum of 1.5%. Analogously, the distribution of the calculated heat power values with respect to the exact ones presents a random trend with all the values (Fig. 11b) within a ± 5% band.

The same behaviour can be observed for the results obtained with the 6-parameter estimation procedure reported in Table 6. Regarding the 4-parameter estimation, Re_1 is not kept fixed, but it is assumed to vary in the range $1.9 \cdot 10^4 < Re_1 < 2.1 \cdot 10^4$ with the number of tests that is increased to 300.

In Figure 12, the coefficients of variation are graphically shown as a function of noise level.

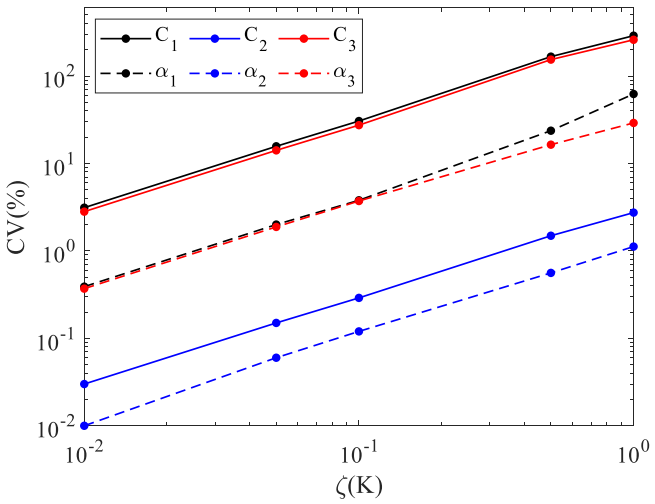

Figure 12. Coefficients of variation for different noise levels for 6-parameter estimation

The estimation of C_2 and α_2 is excellent for all the noise levels and CV values, and confidence intervals are like the ones obtained for the 2-and 4-parameter estimation procedures. C_1, α_1, C_3, α_3 are estimated with success until the noise value of 0.1 K, even if CVs for C_1 and C_3 reach values of 30%. For higher noise values, CI intervals become significantly larger, and CV greatly increases, highlighting the unfeasibility of the estimation of the coefficients of the service fluid sides.

Table 6. Results of parameter estimation on synthetic data (6-parameter case)

Noise level (ζ)	Unknown parameter	exact value	estimated value	CI 95%	CV (%)
0.01	C_1	0.023	0.023	(0.022, 0.025)	3.12
	α_1	0.800	0.798	(0.792, 0.805)	0.39
	C_2	0.023	0.023	(0.023, 0.023)	0.03
	α_2	0.800	0.800	(0.800, 0.800)	0.01
	C_3	0.023	0.023	(0.022, 0.024)	2.81
	α_3	0.800	0.800	(0.794, 0.806)	0.37
0.05	C_1	0.023	0.025	(0.017, 0.032)	15.71
	α_1	0.800	0.793	(0.762, 0.824)	2.00
	C_2	0.023	0.023	(0.023, 0.023)	0.15
	α_2	0.800	0.800	(0.800, 0.801)	0.06
	C_3	0.023	0.025	(0.018, 0.033)	14.11
	α_3	0.800	0.789	(0.760, 0.818)	1.88
0.1	C_1	0.023	0.020	(0.008, 0.031)	30.55
	α_1	0.800	0.816	(0.755, 0.876)	3.79
	C_2	0.023	0.023	(0.023, 0.023)	0.29
	α_2	0.800	0.802	(0.800, 0.804)	0.12
	C_3	0.023	0.029	(0.013, 0.045)	27.40
	α_3	0.800	0.775	(0.718, 0.831)	3.72
0.5	C_1	0.023	0.019	(0.007, 0.131)	166.49
	α_1	0.800	0.811	(0.510, 1.263)	23.69
	C_2	0.023	0.023	(0.022, 0.023)	1.49
	α_2	0.800	0.803	(0.788, 0.805)	0.56
	C_3	0.023	0.027	(-0.05, 0.113)	154.01
	α_3	0.800	0.769	(0.512, 1.006)	16.39
1	C_1	0.023	0.608	(-2.838, 4.054)	289.13
	α_1	0.800	0.469	(-0.103, 1.042)	62.27
	C_2	0.023	0.023	(0.021, 0.024)	2.74
	α_2	0.800	0.804	(0.787, 0.822)	1.12
	C_3	0.023	0.006	(-0.023, 0.035)	259.54
	α_3	0.800	0.944	(0.406, 1.482)	29.06

Even for 6-parameter estimation in Figure 13a, it is reported as the estimation error (Eq. (45)), while in Figure 13b, it is shown as the comparison between the computed values of Q_2 and exact ones regarding the highest noise level (ζ = 1 K).

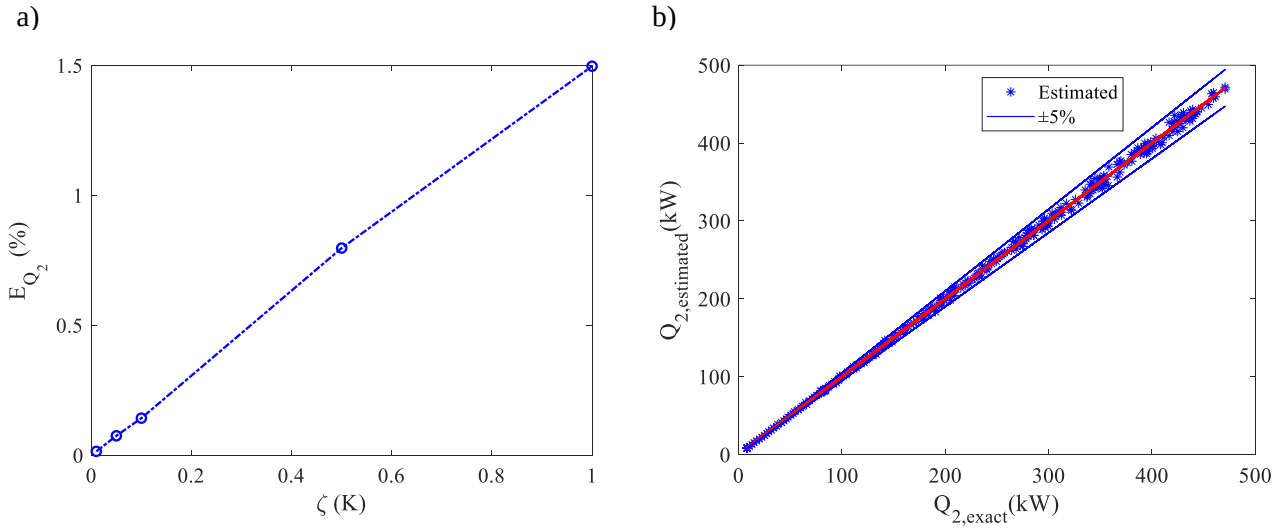

Figure 13. Estimation error E_{Q_2} as a function of the noise level (a) and comparison between exact and estimated heat power Q_2 for noise level ζ = 1 K (b) for the case of 6 parameters estimation

To conclude, also for the 6-parameter approach, the estimation error (Fig. 13a) on the exchanged heat power Q_2 is lower than 1.5%. Moreover, the distribution of the values of calculated heat power of the central annulus with respect to the exact ones (Fig. 13b) has a random spread, and it is included in band of ±5%.

To compare the computational cost of the 2, 4 and 6 parameter estimation procedures in Figure 14, it is reported as the time necessary to find the wanted unknowns for the representative case of $\zeta = 0.1$ K for the three different cases. The adopted calculator is an Intel® Core ™ i3-2120 CPU 3.3GHz with 8GB of RAM memory.

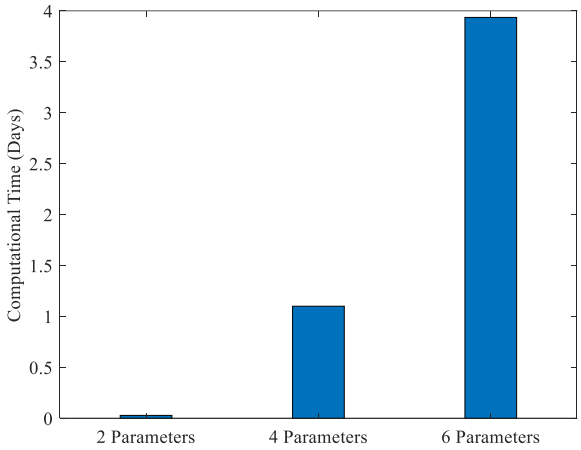

Figure 14. Solution time for the 2, 4 and 6 parameter estimation procedures

The calculation time increases as the number of parameters to be estimated rises. In particular, when going from 2 to 4 parameters, the calculation time increases approximately 38 times (from 41 min. to 26 h), while going from 4 to 6, it increases by 3.6 times (from 26 h to ca. 4 days). Thus, it means that tripling the number of parameters to be estimated causes an increase in 2-order magnitude in the computational time.

Resuming, the assessment of the multiplicative constant C_2 and the Reynolds number exponent α_2 for the product side is obtained with optimal results with the 3 tested approaches for the proposed estimation procedure. Even for the highest noise level ($\zeta = 1$), the confidence intervals and CV are very limited, upholding the effectiveness of the estimation methodology for these parameters.

Furthermore, the 4-and 6-parameter estimation procedures present the advantage of assessing the C and α for the service fluid sides without the necessity of making a priori assumptions.

However, in the case study considered, the estimation of the parameters of the sides of the services (C_1, α_1, C_3, α_3) was found to be feasible only with low noise values ($\zeta \leq 0.1$), while for high noise values ($\zeta \geq 0.5$), 4- and 6-parameter estimation procedures showed an increase in confidence intervals and *CV*s of the estimated coefficients. As mentioned earlier, this weakness for estimating service sides' coefficients at high noise levels is ascribable to the typical food application case studied in this work, in which most of the thermal resistance of the device is due to the contribution of the product side; consequently, it is easier to estimate the coefficients that describe the behaviour of this section than those of the service ones, whose variation does not affect significantly the overall thermal resistance. Moreover, the estimation procedure for 4 and 6 parameters requires more tests than for 2 parameters, increasing the time required for executing the experimental activities. Also, the computational cost of the estimation procedure critically increases with more parameters. This confirms what has been said in paragraph 3 that when talking about parameter estimation procedures, doing all the simplifications that can be reasonably performed can significantly improve the results and reduce the required time and computational costs.

Hence, it is possible to affirm that the 2-parameter estimation procedure is the best one to adopt in most of the working conditions of TTHE, i.e. strictly laminar flow of highly viscous fluid in Section 2 and turbulent flow in Sections 1 and 3, while only when the thermal resistances of the three sections assume comparable values can the 4- and 6-parameter estimation procedure be suggested.

7. Conclusions

This study reports the application of an innovative procedure based on parameter estimation methodology to characterise TTHEs. This investigation is intended to enable the robust estimation of the heat transfer correlation for the product side Nusselt number. The parameter estimation procedure was validated through its

application to both synthetic and experimental data acquired from TTHE for treating highly viscous fluid food. The validation yielded the following results:

- the application of the procedure to synthetic data helped in obtaining an accurate estimation of the unknown coefficients in the product side Nusselt number correlation. Even for the highest noise level considered in this study ($\zeta = 1$ K), the highest value of the coefficient of variation was 4.2%, underlying the very good results achieved.
- the application of the procedure to the experimental data demonstrated that for the product side, the power law dependence of the internal fluid Nusselt number on the Reynolds number can be successfully estimated together with the multiplicative constant. The uncertainty associated with estimating the multiplicative constant C_2 (coefficient of variation of approximately 6.5%) is very low, and the Reynolds number exponent α_2 is determined with a coefficient of variation of approximately 3%.
- the application of the two variants of the procedure (i.e. 4 parameters and 6 parameters) on synthetic data highlighted that, by increasing the number of parameters to be estimated, the coefficients of the product side are still well assessed. However, when most of the thermal resistance of the device is located on the product side, the coefficients of the service sides are well estimated until a low level of noise, while at a high level, their assessment becomes unachievable, making the 2-parameter procedure preferable.
- The application of the two variants of the procedure to synthetic data highlighted that the two variants of the procedure involve an important increase in the time required for executing the experimental activities and an increase in the computational costs, making them the best solution only when the service side thermal resistance is comparable to the product side.

In conclusion, considering the limited effort for the experimental measurements required to apply this estimation procedure (i.e. moderate number of experimental measurements and relatively small computational power and time), the proposed methodology of characterising TTHEs could also represent a effective tool for the producers of this type of device, permitting them to estimate the unknown parameters that are crucial for the design and optimisation of this equipment, which often must be customised to enable specific thermal processes.

Acknowledgements

This work was partially supported by the Emilia-Romagna Region (Piano triennale alte competenze per la ricerca, il trasferimento tecnologico POR FSE 2014/2020). JBT-FoodTech is gratefully acknowledged for setting up the experimental apparatus. The Authors thank Eng. Luigi Tommasiello for his support in the experimental work.

Nomenclature

Symbol	Quantity	SI Unit
A	Heat transfer surface area	m^2
C	Multiplicative constant (Eq. (31))	
$CI^{95\%}$	Confidence interval	
CV	Coefficient of variation	
c_p	Specific heat	kJ/kg·K
D	Diameter	m
h	Convective heat transfer coefficient	$W/m^2 \cdot K$
J^*	Scaled sensitivity coefficient	
$\boldsymbol{J}$	Jacobian operator	
L	Heat exchanger's length	m
$\dot{m}$	Mass flowrate	Kg/s

Nu	Nusselt number	
P_i	Generic unknown parameter	
Pr	Prandtl number	
Q	Heat transfer rate	W
Re	Reynolds number	
R_w	Wall thermal resistance	W/K
S	Target function	
T	Temperature	K
x	Axial coordinate	m
U	Overall heat transfer coefficient	$W/m^2 \cdot K$
W	Wall thickness	m
α	Reynolds number exponent (Eq. (31))	
λ	Fluid thermal conductivity	W/m·K
λ_w	Wall thermal conductivity	W/m·K
σ	Standard error	

Subscripts, superscripts

inlet	Inlet section
outlet	Outlet section

References

[1] Gomaa A., Mohamed M. and Elsaid A.M. (2016). Experimental and Numerical investigation of a triple concentric-tube heat exchanger Appl. Therm. *Eng*. 99 1303.

[2] Garcia-Valladares O. (2004) Numerical simulation of triple concentric-tube heat exchangers Int. J. Therm. Sci. 43 979.

[3] Kumar, P. M. and Hariprasath, V. (2020). A review on triple tube heat exchangers. Materials Today: Proceedings, 21, 584-587.

[4] Tiwari A. K., Javed S., Oztop H. F., Said Z. and Pandya N. S. (2021). Experimental and numerical investigation on the thermal performance of triple tube heat exchanger equipped with different inserts with WO_3/water nanofluid under turbulent condition. Int. J. Therm. Sci. 164, 106861.

[5] Ünal A. (1998). Theoretical analysis of triple concentric-tube heat exchangers part 1: Mathematical modelling. International communications in heat and mass transfer 25 (7), 949–958.

[6] Ünal A. (2003). Effectiveness-ntu relations for triple concentric-tube heat exchanges. International communications in heat and mass transfer 30 (2), 261–272.

[7] Batmaz E. and Sandeep K.P. (2008). Overall heat transfer coefficients and axial temperature distribution in a triple tube heat exchanger. Journal of food process engineering 31 (2), 260–279.

[8] Radulescu S., Negoita I.L. and Onutu I. (2012). Heat transfer coefficient solver for a triple concentric-tube heat exchanger in transition regime. Rev. Chim.(Bucharest) 8, 820–824.

[9] Moya-Rico J. D., Molina A. E., Belmonte J. F., Córcoles Tendero J. I., and Almendros-Ibáñez J. A. (2019). Characterization of a triple concentric-tube heat exchanger with corrugated tubes using Artificial Neural Networks (ANN). Appl. Therm. Eng. 147, 1036–1046.

[10] Bahiraei, M., Mazaheri, N., Hanooni, M. (2021). Performance enhancement of a triple-tube heat exchanger through heat transfer intensification using novel crimped-spiral ribs and nanofluid: A two-phase analysis. Chemical Engineering and Processing - Process Intensification 160,108289.

[11] Bahiraei, M., Kok Foong, L., Hosseini, S., Mazaheri, N. (2021). Neural network combined with nature-inspired algorithms to estimate overall heat transfer coefficient of a ribbed triple-tube heat exchanger operating with a hybrid nanofluid. Measurement: Journal of the International Measurement Confederation 174,108967

[12] Bahiraei, M., Foong, L.K., Hosseini, S., Mazaheri, N. (2021). Predicting heat transfer rate of a ribbed triple-tube heat exchanger working with nanofluid using neural network enhanced by advanced optimization algorithms. Powder Technology 381, 459-476.

[13] Wilson, E.E. (1915). A basis of rational design of heat transfer apparatus. ASME Journal of Heat Transfer 37, 47–70.

[14] Briggs, D.E., Young, E.H. (1969). Modified Wilson plot technique for obtaining heat transfer correlations for shell and tube heat exchangers. Chemical Engineering Progress Symposium Series 65 (92), 35–45.

[15] Khartabil, H.F., Christensen, R.N. (1992). An improved scheme for determining heat transfer correlations from heat exchanger regression models with three unknowns. Experimental Thermal and Fluid Science 5, 808–819.

[16] Styrylska, T.B., Lechowska, A.A. (2003). Unified Wilson plot method for determining heat transfer correlations for heat exchangers. Journal of Heat Transfer –Transactions of the ASME 25, 752–756.

[17] Rose, J.W. (2004). Heat-transfer coefficients, Wilson plots and accuracy of thermal measurements. Experimental Thermal and Fluid Sciences 28 (2–3), 77–86.

[18] Fernández-Seara, J., Uhía, F.J., Sieres, J., Campo, A. (2007). A general review of the Wilson plot method and its modifications to determine convection coefficients in heat exchange devices. Applied Thermal Engineering 27 (17–18), 2745–2757.

[19] Pătrăşcioiu, C. and Rădulescu, S. (2015). Prediction of the outlet temperatures in triple concentric—tube heat exchangers in laminar flow regime: case study. Heat and Mass Transfer, 51(1), 59-66.

[20] Beck, J.V., Arnold, K.J. (1977). Parameter Estimation in Engineering and Science. John Wiley & Sons, New York.

[21] Orlande, H.R., Fudym, O., Maillet, D., & Cotta, R.M. (2011). Thermal measurements and inverse techniques. CRC Press.

[22] Vocale, P., Bozzoli, F., Mocerino, A., Navickaitė, K., & Rainieri, S. (2020). Application of an improved parameter estimation approach to characterize enhanced heat exchangers. International Journal of Heat and Mass Transfer, 147, 118886.

[23] Incropera F.P., DeWitt D.P., Bergman T.L. and Lavine A.S. (2007) Fundamentals of heat and mass transfer 6th ed. (New York: John Wiley & Sons Inc.)

[24] Rainieri, S., Bozzoli, F., Cattani, L. and Vocale, P. (2014). Parameter estimation applied to the heat transfer characterisation of Scraped Surface Heat Exchangers for food applications. Journal of Food Engineering, 125, 147-156.

[25] Blackwell, B. and Beck, J. V. (2010). A technique for uncertainty analysis for inverse heat conduction problems. International Journal of Heat and Mass Transfer, 53(4), 753-759.

[26] Banks, H.T., Holm, K., Robbins, D. (2010). Standard error computations for uncertainty quantification in inverse problems: asymptotic theory vs. bootstrapping. Mathematical and Computer Modelling 52, 1610–1625.

[27] Peacock, S. (1995). Predicting physical properties of factory juices and syrups. International Sugar Journal, 97(1162), 571-2.

[28] Trifirò, A., Bassi, A., Castaldo, D., Bigliardi, D., & Gherardi, S. (1986). Effetti della composizione e della temperatura sulla reologia della purea d'albicocca.

[29] Kozicki, W., Chou, C. H., & Tiu, C. (1966). Non-Newtonian flow in ducts of arbitrary cross-sectional shape. Chemical Engineering Science, 21(8), 665-679.

[30] Taylor, J. R. (1997). Error analysis. Univ. Science Books, Sausalito, California.